



# A Sensitivity Study of a Thermal Propagation Model in an Automotive Battery Module

Chen Huang <sup>\*</sup>, Division of Safety and Transport, RISE Research Institutes of Sweden, Sven Hultins Plats 5, 412 58 Gothenburg, SE, Sweden  
Roeland Bisschop, Battery Optimisation and Monitoring, Volvo Energy, 418 75 Gothenburg, SE, Sweden  
Johan Anderson, Division of Safety and Transport, RISE Research Institutes of Sweden, Sven Hultins Plats 5, 412 58 Gothenburg, SE, Sweden

**Received:** 29 August 2022/**Accepted:** 6 February 2023

**Abstract.** Thermal runaway is a major concern for lithium-ion batteries in electric vehicles. A manufacturing fault or unusual operating conditions may lead to this event. Starting from a single battery cell, more cells may be triggered into thermal runaway, and the battery pack may be destroyed. To prevent this from happening, safety solutions need to be evaluated. Physical testing is an effective, yet costly, method to assessing battery safety performance. As such, the potential of a numerical tool, which can cut costs and reduce product development times, is investigated in terms of capturing a battery module's tolerance to a single cell failure. A 3D-FE model of a battery module was built, using a commercial software, to study thermal runaway propagation. The model assumes that when the cell jelly roll reaches a critical value, thermal runaway occurs. This approach was considered to study the module's tolerance to a single cell failure, which was in reasonable agreement with what had been observed in full-scale experiments. In addition, quantitative sensitivity study on the i) model input parameters, ii) model space, and iii) time resolutions on the computed start time instant and time duration of thermal runaway were performed. The critical temperature was found to have the greatest influence on thermal runaway propagation. The specific heat capacity of jelly roll was found to significantly impact the thermal runaway time duration. The multi-physics model for battery thermal propagation is promising and worth to be applied with care for designing safer batteries in combination with physical testing.

**Keywords:** Lithium-ion battery safety, Thermal runaway, Automotive battery pack, Multi-physics modelling, Sensitivity analysis, Normalized sensitivity coefficient

---

\*Correspondence should be addressed to: Chen Huang, E-mail: [chen.huang@ri.se](mailto:chen.huang@ri.se)



## **1. Introduction**

The lithium-ion battery is a key technology to achieving sustainable and renewable electrical energy. Accordingly, they are increasingly used across various of applications, e.g., energy storage for marine, aerospace, and automotive applications as well as grid-scale Energy Storage Systems (ESS) [1]. Although new technologies present opportunities, they also introduce new risks. For lithium-ion batteries, this entails potential exothermic reactions when the battery is damaged. This may result in a self-sustaining increasing temperature known as thermal runaway.

Thermal runaway in lithium-ion batteries may be catastrophic, even more so if allowed to propagate to other battery cells in an ESS. There has been an increasingly number of incidents reported due to failure of lithium-ion batteries, e.g., an e-bike battery caught on fire and followed by an explosion at a hotel in Vancouver, Canada on June 11th, 2022. A person fell out of the window and lost the life due to the explosion [2]. Two firefighters were killed and one injured when an explosion occurred at a 25 MWh lithium-ion ESS on April 16, 2021, in Beijing, China [3]. Four firefighters received serious injuries when flammable battery gas ignited as they sought entry into an ESS located in Arizona US in 2019 [4]. A total of 27 ESS fire incidents were reported throughout 2017 and 2018 in South Korea [5], causing a significant loss of momentum and reduced further investments in renewable energy [6]. It is thus not only crucial to prevent thermal propagation to save lives, but also to remove the barriers for preventing the usage of renewable energy via batteries.

As temperatures inside the battery increase, various chemical breakdown reactions are triggered which produce more heat and flammable gas [7]. Eventually the battery cell burst and ejects hot and flammable gases. These may self-ignite or be ignited by electrical arcs from the battery as internal short circuits occur. There are several mechanisms that can increase battery cell temperatures or cause internal cell short circuits that can lead to thermal runaway. Specifically, these mechanisms are (i) thermal abuse, e.g., oil spill or a fire incident, (ii) electrical abuse, e.g., overcharge, overdischarge [8], internal and external short circuits, and (iii) mechanical abuse, e.g., nail penetration or crash [9].

Accordingly, the battery thermal runaway process is a multi-physics and multi-scale process [10]. It involves structure mechanics, fluid dynamics, chemical kinetics associated with thermal runaway, heat transfer and combustion, each of which occurs at different time scales. Such a challenging process is commonly studied by physical tests; see recent examples [11–13]. However, experimental tests may be expensive, dangerous, and harmful to the environment. Furthermore, there are many parameters that may affect the battery thermal runaway, such as abuse conditions, battery chemistry, battery aging, battery state of charge, battery form factor (pouch, prismatic, or cylindrical), material properties, and so on. The influence of these parameters and potential safety solutions, can be studied with the help of multi-physics modelling at a substantially lower cost as compared to the experimental approach. At the same time, the models should be calibrated against

experimental data and be carefully applied to the conditions where experimental data is not available.

Recently there has been an exponential increase in publications on battery thermal runaway modelling using different multi-physics tools. The effect of mechanical abuse, i.e., nail penetration was modelled by Zhang et al. [10] by coupling mechanical, electrical, and thermal process, and by Zhao et al. [14]. A battery thermal propagation multi-physics model was built and was calibrated to physical experiments by Larsson et al. [15]. The model was used to study different thermal barriers, i.e., the influence of heat sinks and fire walls between stacked pouch cells, between cells in a battery module. A study on thermal propagation on battery modules was also considered by Feng et al. [16] and Jin et al. [17]. Factors such as overcharging and aging were modelled by Ren et al. [18] and Abada et al. [19], respectively. Wang et al. [20] simulated the factors such as charging C-rate, battery spacing, triggering temperature, on the thermal propagation among battery cells. Hu et al. [21] studied the critical ambient temperature for self-heating of battery cells in different scales using a multi-physics model. An interesting work by García et al. [22] included the models of lithium-ion battery degradation, cooling and thermal runaway kinetics.

This work presents a thermal propagation model for a battery module containing 12 prismatic battery cells based on a 3-Dimensional (3-D) Finite Element (FE) approach. The thermal runaway events were compared with full-scale experiments. Sensitivity studies were carried out to investigate the model parameters as well as the time and space resolutions of the numerical model on the thermal runaway events.

Note that thermal runaway models involving multi-step exothermic reactions [16, 18, 23] solve highly non-linear and stiff partial differential equations, which are computationally expensive [24]. The novelty of this work is to present a short runtime thermal runaway model with the help of full-scale experiments. The calibrated thermal runaway model can be used by researchers and engineers to design safer batteries at low computational cost. Specifically, the thermal runaway model can be used to fast explore the design space by performing parametric studies.

In the next section, the experimental method and setup are briefly summarized. Then, the numerical method and setup are described in Sect. 3. Results and discussions are presented in Sect. 4, followed by the conclusions.

## **2. Experimental Method and Setup**

The thermal runaway experiments were performed at RISE during 2019 within the framework of a research project for evaluating the performance of fixed fire suppression system in controlling thermal runaway events [11]. The tested battery pack consisted of two live battery modules and six dummy modules. One live battery module contained 12 hard prismatic cells with anode and cathode material being C/NMC, nominal voltage being 3.7 V, and rated capacity being 28 Ah, respectively. Sand was filled in the dummy battery module and sealed. The case of dummy module was made of stainless steel. A circular opening of 24 mm in diam-

eter on the body of the battery pack was made to expose a battery cell directly to a gas burner (see Fig. 1a). This test setup aimed at simulating thermal propagation in case of a fire. Note that only one test was performed using two-layer battery packs (see Fig. 1), and the rest of the tests were performed using one-layer battery pack. The reason is that the risk for fire propagation from the upper to the lower layer was low. In all tests the state of charge of batteries was 100%, which is expected to be a conservative case.

### 3. Numerical Method and Setup

Thermal runaway means the exothermic reactions in the battery are out of control, resulting in a fast release of aerosol droplets from electrolyte [25], as well as flammable and toxic gases, with the increase of temperature and pressure inside the battery [26]. The battery thermal runaway process is a multi-physics and multi-scale process, which includes (i) thermal runaway chemical reactions, (ii) heat transfer inside of the battery module and pack via heat conduction, convection and radiation, (iii) flammable and toxic gas release, (iv) ignition and burning of the gas and so on. In this work, we focus exclusively on the thermal runaway propagation on the module level, i.e., thermal runaway spreading from one cell to the next, inside a battery module.

#### 3.1. Numerical Method

A heat transfer model using 3-D FE approach is adopted with a combination of control logics and an empirical model of thermal runaway, which will be described later, using a commercial program GT-SUITE version-2021 [27]. The governing equation for the heat transfer model is written as follows



(a) experimental setup



(b) thermal runaway event during a free burn test.

**Figure 1. The automotive battery pack with a gas burner for heating one of the battery cells.**

## A Sensitivity Study of a Thermal Propagation Model

$$\rho_{jr}c_{p,jr}\frac{dT}{dt} - \nabla \cdot (k\nabla T) = \sum \dot{Q}_{sur} + \sum \dot{Q}_{gen} \quad (1)$$

where  $\rho_{jr}$ ,  $c_{p,jr}$  and  $k$  are the density, specific heat capacity and the conductivity of the jelly roll, respectively.  $\dot{Q}_{sur}$  is the heat transfer rate between the battery and the surrounding through conduction, convection, radiation, and venting of gas.  $\dot{Q}_{gen}$  is the internal heat generation rate of lithium-ion battery during thermal runaway.

The knowledge gap remains in fully understanding the battery thermal runaway process [9]. Moreover, to reduce computational cost associated with solving multi-step thermal decomposition reactions, a thermal runaway model based on an empirical approach by assuming a constant heat generate rate during thermal runaway is adopted. Furthermore, the thermal runaway event is assumed to be triggered when the averaged battery cell temperature reaches a critical value  $T_{cr}$ .

The heat transfer model invokes material thermophysical properties, such as thermal conductivity, specific heat capacity and contact conductance. Since there was no electric current flowing in the battery pack during the test, the battery cells are modelled solely from a thermal standpoint.

Figure 2 shows the geometric configuration of the battery module containing 12 hard prismatic cells and bus connectors. Following the settings in a previous study [28], a heat rate being equal to 480 W or a heat flux being equal to 1061 kW/m<sup>2</sup> is assumed to be applied to the heating area (see Fig. 2) on cell number 6 to initiate the thermal runaway process. Once the average temperature of a cell jelly roll reaches a critical value, i.e.,  $T_{cr} = 443$  K, the battery cell releases heat at a constant value of 1.8 kW for 20 s. This corresponds to a total energy in a battery cell being 450 kJ [28] and 56% of energy heats up the battery cell.

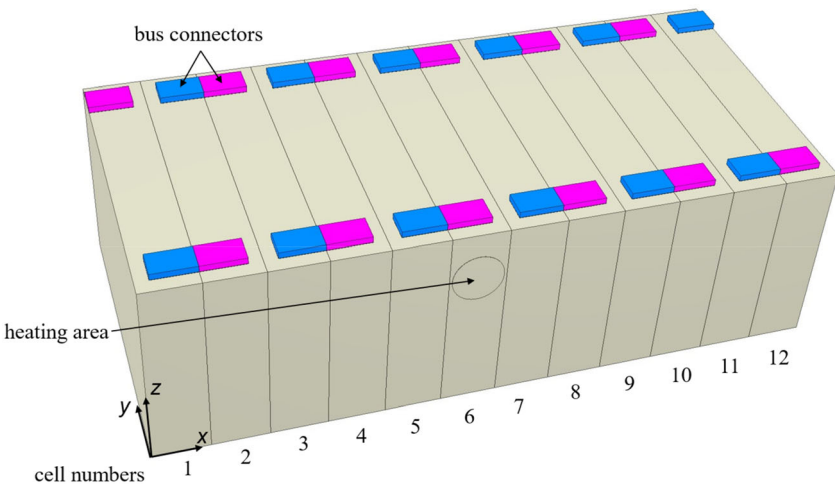


**Figure 2. Geometry of the battery module including 12 prismatic cells and bus connectors in the simulations.**

### 3.2. Numerical Model Setup

**3.2.1. Material Thermophysical Properties and Model Parameters** Since the focus of this work is to study the thermal propagation among the battery cells, the detailed geometry of the battery module and pack was not modelled. Instead, one battery module consisting of 12 hard prismatic cells and bus connectors were modelled using 3-D FE approach. The battery module including cell casings, jelly rolls and bus connectors is shown in Fig. 2. The cells are assumed to be connected in series with anode marked in magenta and cathode marked in blue. The complete model consists of 58 663 tetrahedral elements. One simulation took 25 min (CPU time) for a simulation duration of 40 min on a laptop with Intel Core i7-7820 HQ CPU and 32 GB RAM. The battery cell casing was modelled as 1 mm thick Aluminium material, and the bus connectors were modelled as Aluminium material as well. The cell jelly roll was composed of materials such as anode, separator, cathode, and electrolyte, etc. The battery jelly roll was treated as anisotropic material in terms of thermal conductivity with 0.2 W/(m·K) in  $x$  direction and 32 W/(m·K) in  $y$  and  $z$  directions [29] (see Fig. 2). A summary of the thermophysical properties for the model components is shown in Table 1.

The components were assumed in direct contact with each other; therefore, thermal contact conductance was specified. Thermal contact conductance depends on multiple factors such as the materials in contact with each other, the roughness of the surfaces and the pressure between the surfaces. The thermal contact conductance used in this work is shown in Table 2.

**3.2.2. Initial and Boundary Conditions** Initial and boundary conditions of the model were assumed due to the lack of measurement data. The initial temperature on the components was 300 K in the simulations. The temperature on the bound-

**Table 1**  
**Summary of Thermophysical Properties of Different Components in the Battery Pack**

Component	Material	Density $\rho$ [kg/m <sup>3</sup> ]	Thermal conductivity $k$ [W/(m·K)]	Specific heat capacity $c_p$ [J/(kg·K)]	Source
Cell casing and bus connectors	Aluminium	2702	237 at 300 K, 218 at 800 K	903 at 300 K, 1146 at 800 K	GT-SUITE v-2021 material library [27]
Cell jelly roll	Combined material including anode, separator, cathode and electrolyte, etc	2800	Anisotropic 0.2 in $x$ direction, 32 in $y$ and $z$ directions (see directions in Fig. 2)	830	Drake et al. [29], Richard and Dahn [30]

**Table 2**  
**Summary of Contact Conductance for Heat Conduction Between Components**

Surfaces in contact with each other	Contact conductance $h_c$ [W/(m <sup>2</sup> ·K)]	Source
Jelly roll to casing	670	Gaitonde et al. [31]
Casing to casing	2000	Not available

aries was set being 300 K with an external heat transfer correlation activated in GT-SUITE for evaluating Nusselt number  $Nu$  as follows

$$Nu = 0.037Re^{0.8}Pr^{0.333} \quad (2)$$

where,  $Re$  is the Reynolds number, evaluated using ambient velocity  $u$  and reference length  $L$ ;  $Pr$  is the Prandtl number. The ambient velocity  $u$  was set being 1 m/s for all boundaries, whereas the reference length  $L$  was set being 150 mm for left and right boundaries, and 320 mm for the rest of the boundaries, respectively (see Fig. 2). Such an approach means convective heat transfer coefficients, depend on the ambient flow condition [27].

### 3.3. Normalized Sensitivity Coefficients

Two parameters were analysed, the start time instant of the first battery cell going into thermal runaway and the duration for all 12 battery cells going into thermal runaway. The sensitivity coefficients  $\partial y_j / \partial x_i$  for different parameters and on different results are incomparable due to different units. A solution is to introduce a normalized sensitivity coefficient following the work of Turányi [32] and Chaudhari and Stoliarov [33] as follows

$$\tilde{S} = \frac{\partial y_j}{\partial x_i} \frac{x_i}{y_j} \quad (3)$$

where,  $x$  is an input parameter; and  $y$  is the computed result; the subscript  $i$  corresponds to the  $i$ -th input parameter; the subscript  $j$  corresponds to the  $j$ -th result. The normalized sensitivity coefficient represents a fractional change in  $y$  caused by a fractional change in  $x$ . It can be inferred from Eq. 3 that a positive normalized sensitivity coefficient means that an increase in  $x$  results in an increase in  $y$ , and vice versa.

## 4. Results and Discussions

### 4.1. Comparison with Experiments

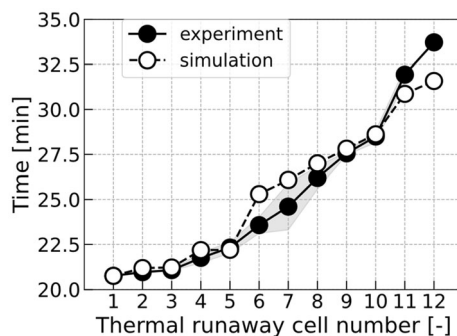
The comparison between simulations and experiments was focused on the development of thermal runaway events of the cells, i.e., the thermal runaway time

instants with respect to the accumulated number of cells which went thermal runaway (see Fig. 3). Note that the experimental data was based on visual observations of two tests, whereas in the simulations the thermal runaway time instants are defined when the average temperature in the cell jelly roll is above a critical temperature of 443 K. The filled symbols in Fig. 3 are the averaged value of two test observations and the grey area represents the standard derivation based on those two tests. In the experiments the thermal runaway was observed after the gas burner had been heating the battery module for roughly 20 min. In line with the experiments, the simulation showed that the time instant for the first cell which went into thermal runaway was 20.75 min.

Table 3 plots the calculated temperature fields at different time instants for the views of the whole battery pack and the section view of a plan cutting through the middle of the battery pack perpendicular to the  $y$ -axis (see Fig. 2). Note the white net on the temperature plots are the computational mesh. The temperature plots show that at the time instants 21, 26, 30, and 32 min, the corresponding cells went into thermal runaway are cell numbers 4 to 6, cell numbers 2 to 9, cell numbers 1 to 10 and all the cells, respectively.

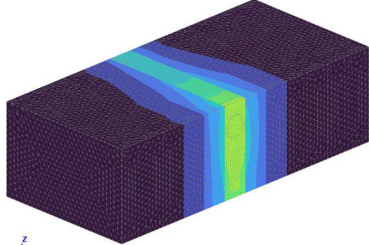
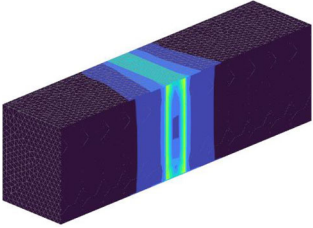
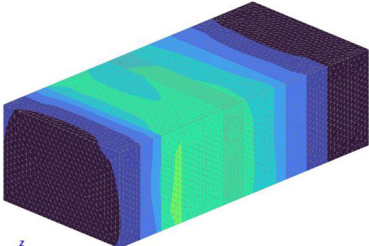
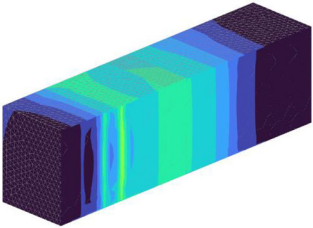
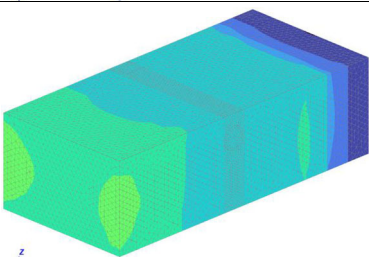
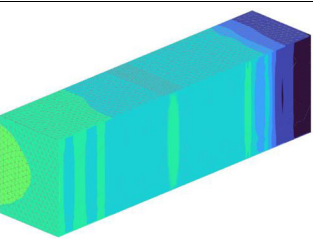
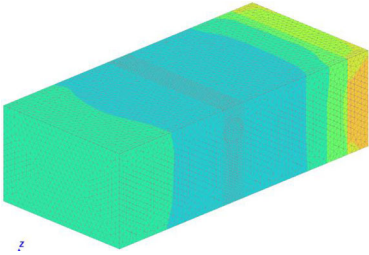
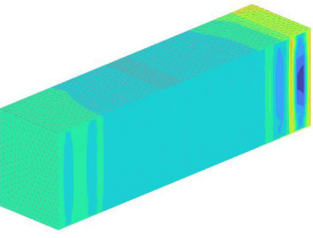
## 4.2. Sensitivity Analysis of Thermal Wall Calculation Interval and Grid Resolution

4.2.1. *Effect of Thermal Wall Calculation Interval* The thermal wall calculation interval  $\Delta t$  in GT-suite controls how often the heat transfer equations are solved. A sensitivity study of varying the thermal wall calculation interval from 1 s to 3 s on the computed results are shown in Fig. 4. Figure 4 shows that a thermal wall calculation interval of 2 s is an optimum choice when balancing between CPU time and the accuracy of the solution for the current case. Too large thermal wall calculation interval, i.e., 3 s, cannot accurately capture the transient behaviour of



**Figure 3. Comparison between the experiments and simulations of the time instants versus the number of cells which go into thermal runaway. The grey area represents the standard derivation based on the experiments.**

**Table 3**  
**Calculated Temperature Ffields at Different Time Instants**

Time instants [min]	Calculated temperature field, whole pack	Calculated temperature field, slice view
21		
26		
30		
32		
Temperature scale [K]		

the thermal propagation process. Note that the CPU time is proportional to the reciprocal of the thermal wall calculation interval.

**4.2.2. Effect of Grid Resolution** Three types of grids were tested with names fine, finer, and finest, respectively (see Table 4 for detailed characterization of the grid size). Shown in Fig. 5 is the effect of grid resolution  $\Delta x$  on the computed results. The finest grid yields a slightly slower thermal runaway process especially at the end. At the same time, the computational cost increases substantially (see Table 4). A fine grid is used in all the rest of the simulations with a compromise between the accuracy and the computational cost.

**4.3. Sensitivity Analysis of Model Parameters**

Due to the lack of measurement data of battery cell thermophysical properties and the fundamental understanding of the thermal runaway phenomena, the model parameters were either taken from the literature or estimated. At the same

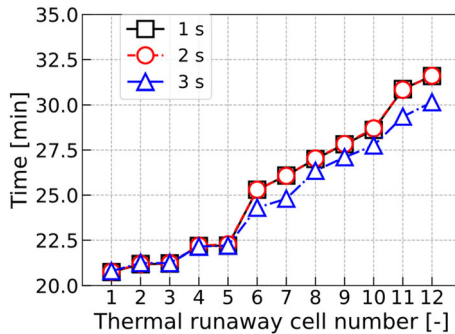


**Figure 4. Calculated thermal runaway time instants versus thermal runaway cell number for different thermal wall calculation intervals.**

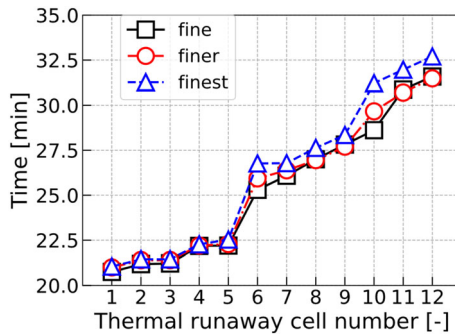


**Figure 5. Calculated thermal runaway time instants versus thermal runaway cell number for different grid resolutions  $\Delta x$ .**

**Table 4**  
**Parameters of the Three Types of Grids**

Name	Grid size [mm]	Total number of elements [-]	CPU time
Fine	2.5 to 10	58 663	25 min
Finer	2 to 7	101 942	1 h 19 min
Finest	1.25 to 5	201 736	3 h 36 min

**Table 5**  
**Parameters Used in the Sensitivity Analysis**

Parameters	Critical temperature $T_{cr}$ [K]	Thermal contact conductance between jelly roll and cell casing $h_{c,jr}$ [W/(m <sup>2</sup> ·K)]	Thermal contact conductance between cell casings $h_{c,cc}$ [W/(m <sup>2</sup> ·K)]	Total energy released from a battery cell $\Delta H$ [kJ]	Specific heat capacity of jelly roll $c_{p,jr}$ [J/(kg·K)]
Values with variations	443 ± 10	670 ± 335	2000 ± 1000	450 ± 22.5	830 ± 41.5

time, the values of battery cell thermophysical properties differ substantially in the literature. For example, the difference of jelly roll heat capacity in Richard and Dahn [30] and Jin et al. [17] is 33%. Furthermore, the difference of jelly roll heat conductivity in Drake et al. [29] and Jin et al. [17] is 52%. It is therefore important to quantify the sensitivity of model input parameters to the computed results. Five model input parameters and their variations are listed in Table 5. The computed thermal runaway time instant versus thermal runaway cell number is shown in Fig. 6 for different model input parameters. Note figure legend “medium” in Fig. 6 represents the default values plus and minus the variation value in Table 5, respectively. Energy release duration for the thermal runaway and jelly roll thermal conductivity have negligible influence on the computed thermal runaway time instants. Therefore, the results are not shown here.

To further compare the effects of the model input parameters on the computed results, i.e., the start time instant of the first battery cell going into thermal runaway and the duration for all 12 battery cells going into thermal runaway, normalized sensitivity coefficients defined in Eq. (2) are calculated. Note the normalized sensitivity coefficients are calculated for model input parameters, except for the energy release time in Table 5 as well as  $\Delta t$  and  $\Delta x$ . Figure 7 shows the normalized sensitivity coefficients for the start time instant of the first battery cell going into thermal runaway and the normalized sensitivity coefficients for the duration for all 12 battery cells going into thermal runaway. A positive value of normalized sensitivity coefficient means that a fractional increase in the input

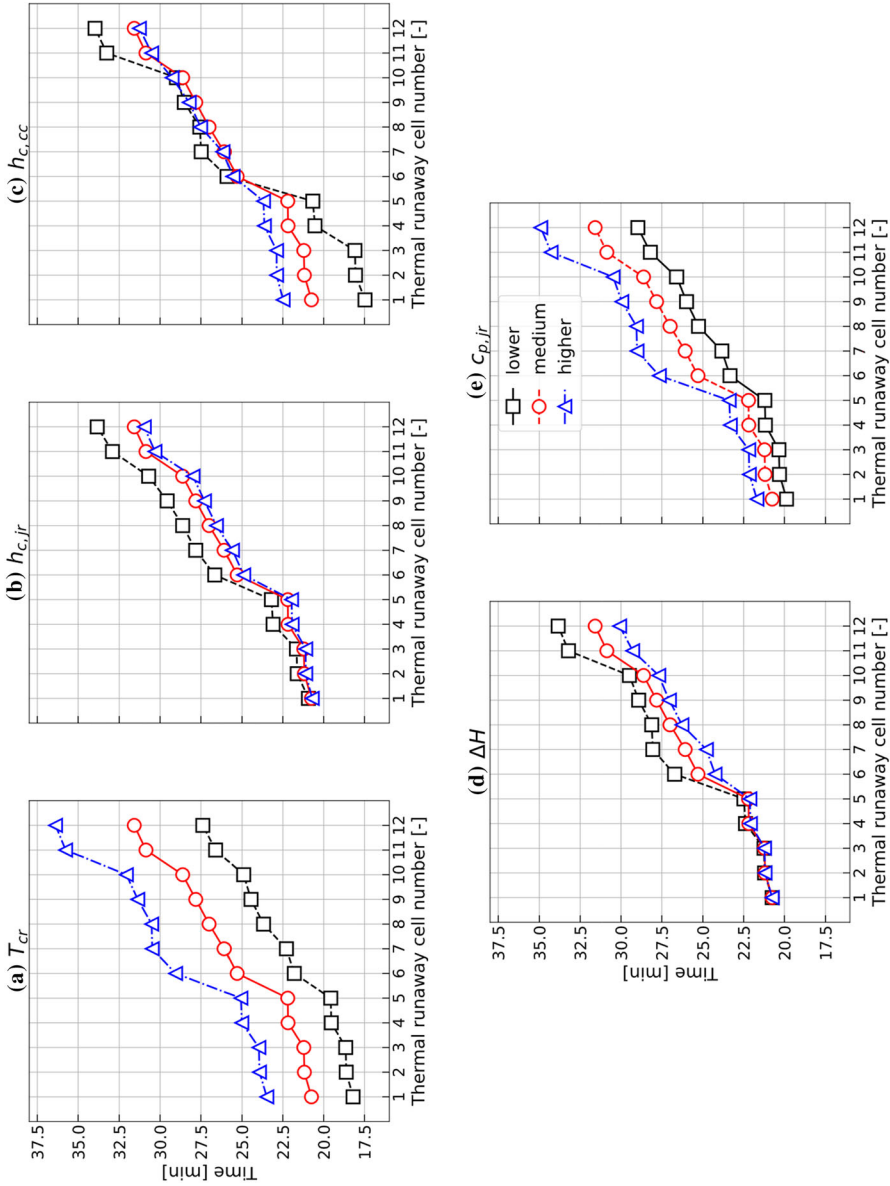


**Figure 6. Thermal runaway time instants versus thermal runaway cell number for different model parameters. Note the legend on subfigure (e) is valid for all subfigures.**

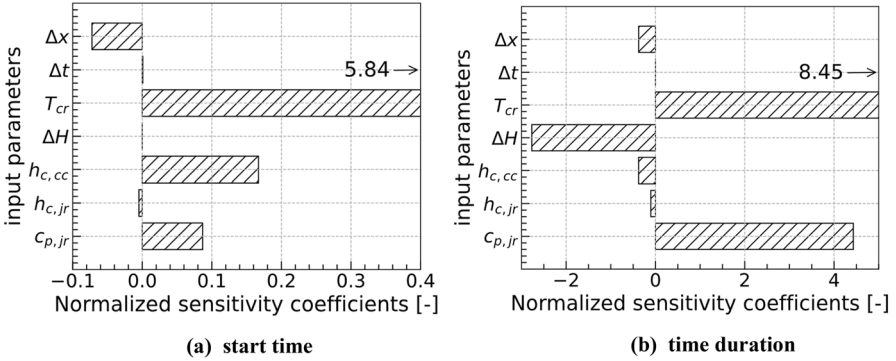


**Figure 7. Normalized sensitivity coefficients for the start time instant of the first battery cell going into thermal runaway and the duration for all 12 battery cells going into thermal runaway for different input parameters.**

parameter increases the results, and vice versa. Figure 7 shows that the critical temperature  $T_{cr}$  has the largest influence on the thermal runaway process. A higher  $T_{cr}$  yields a delayed thermal runaway and a longer thermal runaway duration. In addition, a higher specific heat capacity of jelly roll  $c_{p,jr}$  yields a delayed thermal runaway and a longer runaway duration. Furthermore, a higher thermal contact conductance between cell casings  $h_{c,cc}$  shortens the initiation of thermal runaway, whereas a higher total energy released from a battery cell  $\Delta H$  shortens the thermal runaway duration.

## 5. Conclusions

A battery thermal runaway model containing 12 prismatic cells based on 3-D FE approach with a combination of control logics and an empirical model of thermal runaway was built using a commercial multi-physics software. The computed thermal runaway time instants versus thermal runaway cell number were compared with full-scale experimental data with reasonable agreement. Quantitative sensitivity study on the model input parameters and model space and time resolutions on the computed start time instant and time duration of thermal runaway were performed. The critical temperature  $T_{cr}$  was found to have the largest influence on the thermal runaway process. The specific heat capacity of the jelly roll  $c_{p,jr}$  was found to have significant influence on the thermal runaway time duration. The multi-physics model for battery thermal runaway process is promising and worth to be applied with care for designing safer batteries in combination with full-scale testing.

## **Acknowledgements**

The authors would like to acknowledge Brandforsk (Grant Number 322-001) and Batterisäkerhet project at Safety and Transport division at RISE for financial support of this project. Jonathan Harrison a former application engineer at Gamma Technologies is especially acknowledged for the initiation of interest in this research topic. Dig Vijay at Gamma Technologies is acknowledged for the professional technical support with great patience. Alastair Temple at RISE is acknowledged for valuable comments.

## **Funding**

Open access funding provided by RISE Research Institutes of Sweden. This study is supported by the Brandforsk (Grant No. 322-001) and Johan Anderson, RISE Research Institutes of Sweden AB.

## **Declarations**

**Conflict of interest** The authors declare that they have no known competing financial interests or personal relationships that could have appeared to influence the work reported in this paper.

## **Open Access**

This article is licensed under a Creative Commons Attribution 4.0 International License, which permits use, sharing, adaptation, distribution and reproduction in any medium or format, as long as you give appropriate credit to the original author(s) and the source, provide a link to the Creative Commons licence, and indicate if changes were made. The images or other third party material in this article are included in the article's Creative Commons licence, unless indicated otherwise in a credit line to the material. If material is not included in the article's Creative Commons licence and your intended use is not permitted by statutory regulation or exceeds the permitted use, you will need to obtain permission directly from the copyright holder. To view a copy of this licence, visit <http://creativecommons.org/licenses/by/4.0/>.

## **References**

1. Zubi G, Dufo-López R, Carvalho M, Pasaoglu G (2018) The lithium-ion battery: State of the art and future perspectives. *Renew Sust Energ Rev* 89:292–308. <https://doi.org/10.1016/j.rser.2018.03.002>

## *A Sensitivity Study of a Thermal Propagation Model*

2. CTV news (2022) Lithium ion batteries ‘number one’ cause of fire-related deaths in Vancouver, officials say. [https://beta-ctvnews-ca.cdn.ampproject.org/c/s/beta.ctvnews.ca/local/british-columbia/2022/6/13/1\\_5945475.amp.html](https://beta-ctvnews-ca.cdn.ampproject.org/c/s/beta.ctvnews.ca/local/british-columbia/2022/6/13/1_5945475.amp.html). Accessed 30 June, 2022
3. CTIF (2021) Accident analysis of the Beijing lithium battery explosion which killed two firefighters. <https://ctif.org/news/accident-analysis-beijing-lithium-battery-explosion-which-killed-two-firefighters>. Accessed 30 June, 2022
4. McKinnon MB, DeCrane S, Kerber S (2020) Four firefighters injured in lithium-ion battery energy storage system explosion—Arizona. UL Firefighter Safety Research Institute, Columbia, MD 20145
5. Bosa Energy (2019) Lessons we learn from 27 Energy storage systems fires in Korea: LFP might be the right choice. <http://www.bosaenergy.com/home-newsinfo-id-19.html>. Accessed 30 June, 2022
6. The Korea Times (2018) Frequent fire raising concerns over safety of solar energy, [http://www.koreatimes.co.kr/www/tech/2018/12/133\\_260560.html](http://www.koreatimes.co.kr/www/tech/2018/12/133_260560.html). Accessed 30 June, 2022
7. Sun P, Bisschop R, Niu H, Huang X (2020) A review of battery fires in electric vehicles. *Fire Technol* 56:1361–1410. <https://doi.org/10.1007/s10694-019-00944-3>
8. Feng X, Ouyang M, Liu X, Lu L, Xia Y, He X (2018) Thermal runaway mechanism of lithium ion battery for electric vehicles: a review. *Energy Storage Mater* 10:246–267. <https://doi.org/10.1016/j.ensm.2017.05.013>
9. Wang Q, Mao B, Stolarov SI, Sun J (2019) A review of lithium ion battery failure mechanisms and fire prevention strategies. *Prog Energy Combust Sci* 73:95–131. <https://doi.org/10.1016/j.peccs.2019.03.002>
10. Zhang C, Santhanagopalan S, Sprague MA, Pesaran AA (2015) Coupled mechanical-electrical-thermal modeling for short-circuit prediction in a lithium-ion cell under mechanical abuse. *J Power Sources* 290:102–113. <https://doi.org/10.1016/j.jpowsour.2015.04.162>
11. Bisschop R, Willstrand O, Rosengren M (2020) Handling lithium-ion batteries in electric vehicles: preventing and recovering from hazardous events. *Fire Technol* 56:2671–2694. <https://doi.org/10.1007/s10694-020-01038-1>
12. Wang Z, He T, Bian H, Jiang F, Yang Y (2021) Characteristics of and factors influencing thermal runaway propagation in lithium-ion battery packs. *J. Energy Storage* 41:102956. <https://doi.org/10.1016/j.est.2021.102956>
13. Yan W, Wang Z, Chen S (2021) Quantitative analysis on the heat transfer modes in the process of thermal runaway propagation in lithium-ion battery pack under confined and semi-confined space. *Int. J. Heat Mass Transf.* 176:121483. <https://doi.org/10.1016/j.ijheatmasstransfer.2021.121483>
14. Zhao R, Liu J, Gu J (2016) Simulation and experimental study on lithium ion battery short circuit. *Appl Energy* 173:29–39. <https://doi.org/10.1016/j.apenergy.2016.04.016>
15. Larsson F, Anderson J, Andersson P, Mellander B-E (2016) Thermal modelling of cell-to-cell fire propagation and cascading thermal runaway failure effects for lithium-ion battery cells and modules using fire walls. *J Electrochem Soc* 163(14):A2854–A2865. <https://doi.org/10.1149/2.0131614jes>
16. Feng X, Lu L, Ouyang M, Li J, He X (2016) A 3D thermal runaway propagation model for a large format lithium ion battery module. *Energy* 115(Part 1):194–208. <https://doi.org/10.1016/j.energy.2016.08.094>
17. Jin C, Sun Y, Wang H, Zheng Y, Wang S, Rui X, Xu C, Feng X, Wang H, Ouyang M (2022) Heating power and heating energy effect on the thermal runaway propagation characteristics of lithium-ion battery module: experiments and modeling. *Appl. Energy* 312:118760. <https://doi.org/10.1016/j.apenergy.2022.118760>

18. Ren D, Feng X, Lu L, Ouyang M, Zheng S, Li J, He X (2017) An electrochemical-thermal coupled overcharge-to-thermal-runaway model for lithium ion battery. *J Power Sources* 364:328–340. <https://doi.org/10.1016/j.jpowsour.2017.08.035>
19. Abada S, Petit M, Lecocq A, Marlair G, Sauvant-Moynot V, Huet F (2018) Combined experimental and modeling approaches of the thermal runaway of fresh and aged lithium-ion batteries. *J Power Sources* 399:264–273. <https://doi.org/10.1016/j.jpowsour.2018.07.094>
20. Wang W, He T, He S, You T, Khan F (2021) Modeling of thermal runaway propagation of NMC battery packs after fast charging operation. *Process Saf Environ Prot* 154:104–117. <https://doi.org/10.1016/j.psep.2021.08.006>
21. Hu Z, He X, Restuccia F, Yuan H, Rein G (2021) Numerical study of scale effects on self-heating ignition of lithium-ion batteries stored in boxes, shelves and racks. *Appl. Therm. Eng.* 190:116780. <https://doi.org/10.1016/j.applthermaleng.2021.116780>
22. García A, Monsalve-Serrano J, Sari RL, Martínez-Boggio S (2022) Thermal runaway evaluation and thermal performance enhancement of a lithium-ion battery coupling cooling system and battery sub-models. *Appl. Therm. Eng.* 202:117884. <https://doi.org/10.1016/j.applthermaleng.2021.117884>
23. Kim GH, Pesaran A, Spotnitz R (2007) A three-dimensional thermal abuse model for lithium-ion cells. *J Power sources* 170(2):476–489. <https://doi.org/10.1016/j.jpowsour.2007.04.018>
24. Parhizi M, Jain A, Kilaz G, Ostanek JK (2022) Accelerating the numerical solution of thermal runaway in Li-ion batteries. *J. Power Sources* 538:231531. <https://doi.org/10.1016/j.jpowsour.2022.231531>
25. Harris SJ, Timmons A, Pitz WJ (2009) A combustion chemistry analysis of carbonate solvents used in Li-ion batteries. *J Power Sources* 193:855–858. <https://doi.org/10.1016/j.jpowsour.2009.04.030>
26. Wang Q, Ping P, Zhao X, Chu G, Sun J, Chen C (2012) Thermal runaway caused fire and explosion of lithium ion battery. *J Power Sources* 208:210–224. <https://doi.org/10.1016/j.jpowsour.2012.02.038>
27. Gamma Technologies, 2021. GT-SUITE version-2021 build 3
28. Bisschop R, Harrison J, Huang C (2021) Using multi-physics software to model thermal runaway propagation in automotive battery packs. In: The 2nd International Symposium on Lithium Battery Fire Safety, 31 October to 3 November 2021, Hefei, China
29. Drake SJ, Wetz DA, Ostanek JK, Miller SP, Heinzl JM, Jain A (2014) Measurement of anisotropic thermophysical properties of cylindrical Li-ion cells. *J Power Sources* 252:298–304. <https://doi.org/10.1016/j.jpowsour.2013.11.107>
30. Richard M, Dahn J (1999) Accelerating rate calorimetry study on the thermal stability of lithium intercalated graphite in electrolyte. I. *Exp J Electrochem Soc* 146:2068
31. Gaitonde A, Nimmagadda A, Marconnet A (2017) Measurement of interfacial thermal conductance in Lithium ion batteries. *J Power Sources* 343:431–436. <https://doi.org/10.1016/j.jpowsour.2017.01.019>
32. Turányi T (1997) Applications of sensitivity analysis to combustion chemistry. *Reliab Eng Syst Saf* 57:41–48
33. Chaudhari DM, Stoliarov SI (2022) Analysis of sensitivity of vertical corner flame spread dynamics to uncertainties in the model input. In: The 10th International Seminar on Fire and Explosion Hazards, 22 to 27 May 2022, Oslo